

Estimation of errors on the PSF reconstruction process for myopic deconvolution

Exposito J.^a, Gratadour D.^a, Clénet Y.^a, Rousset G.^a and Mugnier L.^b.

^a LESIA, Observatoire de Paris, CNRS, UPMC, Université Paris-Diderot, 5 place Jules Janssen, 92195 Meudon, France

^b ONERA - The French Aerospace Lab, F-92322 Châtillon, France

ABSTRACT

Images obtained with adaptive optics (AO) systems can be improved by using restoration techniques, the AO-correction being only partial. However, these methods require an accurate knowledge of the system point spread function (PSF). Adaptive optics systems allow one to estimate the point spread function (PSF) during the science observation. Using data from the wave-front sensor (WFS), a direct estimation of the averaged parallel phase structure and an estimation of the noise on the measurements are provided. The averaged orthogonal phase structure (not seen by the system), and the aliasing covariance are estimated using an end-to-end AO simulation. Finally, the estimated PSF is reconstructed using the algorithm of Véran et al. (1997).¹ However, this reconstruction is non perfect. Several approximations are done (stationary residual phase, gaussian phase, simulated aliasing, etc...) and can impact the optical transfer function (OTF) in the case of a rather poor correction. Our aim is to give an error budget for the whole PSF reconstruction process and to link this PSF reconstruction with a deconvolution algorithm that take into account this PSF variability. Indeed, a myopic deconvolution algorithm can be feed with a priori on the object and the PSF. The latter can be obtained by studying the PSF reconstruction error budget as follows in this paper. Finally, this work will lead to an estimation of the error on the deconvolved image allowing one to perform an accurate astrometry/photometry on the observed objects and to strengthen the contrast in the images. We concluded that to neglect the global cross-term or to estimate the aliasing on the measurements using simulations has no effect on the PSF reconstruction.

Keywords: PSF reconstruction, deconvolution, adaptive optics, image processing

1. INTRODUCTION

For large ground-based telescope, the main contributor to the optical aberrations is the atmospheric turbulence. Adaptive optics (AO) is used to correct these aberrations : the wave-fronts are measured and corrected in real time by a deformable mirror whose shape is updated to match the instantaneous atmospheric aberrations. The performance of the system is never perfect. A residual halo still affect the long exposure point spread function (PSF). As a consequence, the contrast of the fine structures of an object is reduced. The common way to restore the contrast is to use a deconvolution algorithm. These methods require a rather good estimation of the PSF. For AO imaging, the long exposure PSF depends on the performances of the system during the observation. These performances fluctuate in time. As a consequence, the PSF is variable.

The AO PSF can be estimated if a star is present close to the object, but this configuration is exceptional. Another way to obtain the PSF during the observation is to use the data from the AO loop : the wave-front sensor (WFS) measurements and the commands sent to the deformable mirror (DM). This method was developed by Véran et al. (1997),¹ the advantage is to provide an estimation of the PSF synchronized with the scientific data acquisition so that the temporal variability is not a problem. However, to reconstruct the PSF, several approximations are done.

In this paper, we present our study about the main approximations related to a Shack-Hartmann WFS, based on the work of Véran et al. (1997). We try to estimate the validity and the errors caused by these

Further author information: (Send correspondence to J. Exposito)

J. Exposito: E-mail: jonathan.expositocano@obspm.fr, Telephone: +33 (0)1 45 07 71 78

approximations on the estimation of the optical transfer function (OTF). The future aim of this study is to give an error budget during the whole reconstruction process and the feed of a myopic deconvolution algorithm to get the best estimation of the restored object.

2. LONG EXPOSURE PSF

2.1 Image formation

The formation of images in the focal plane of a telescope is totally spatially characterized by its PSF. The wave-front in the telescope is diffracted by the pupil and its complex amplitude in the focal plane is given by:

$$\Psi_{im}(\vec{\alpha}) = \int \Psi(\vec{x})P(\vec{x}) \exp\left[-\frac{2i\pi}{\lambda}\vec{x}\vec{\alpha}\right]d\vec{x} \quad (1)$$

Where $\Psi(\vec{x})$ is the complex incident wave-front, $P(\vec{x})$ is the pupil function, λ the observed wavelength, \vec{x} the spatial coordinate in the pupil and $\vec{\alpha}$ the angular coordinate in the focal plane. The PSF is the square modulus of the Fourier transform of the pupil.

Without any turbulence or aberration, $\Psi(\vec{x}) = 1$. In the frequency plane, the system is totally characterized by its OTF that is defined by the autocorrelation of the wave-front in the telescope pupil:

$$\vec{B}(\vec{\rho}) = \frac{1}{S} \int \Psi(\vec{x})\Psi^*(\vec{x} + \vec{\rho})P(\vec{x})P^*(\vec{x} + \vec{\rho})d\vec{x} \quad (2)$$

Where S is the surface of the pupil. For a circular pupil, the autocorrelation gives a cut-off frequency at D/λ . In astronomy imaging, the wave-front is a plane wave. However, the wave-front is affected passing through the atmosphere, leading, in the image, to a cut-off frequency $\frac{r_0}{\lambda}$ lower than the theoretical one ($\frac{D}{\lambda}$) and thus a blurred image in the focal plane.

2.2 Long exposure PSF without AO

The variations of the density in the atmosphere generate some variations of the refractive index (Roddier 1981²). These variations cause the deformation of the wave-front that is now written:

$$\Psi(\vec{x}) = |\psi(\vec{x})| \exp[-i\phi(\vec{x})] \quad (3)$$

Considering the near-field assumption, the amplitude variations (twinkling) can be neglected such that the wave-front is:

$$\Psi(\vec{x}) = \exp[-i\phi(\vec{x})] \quad (4)$$

Using the Eq. 2 for the atmospheric turbulence, the long exposure OTF of the system can be written:

$$\langle \vec{B}(\vec{\rho}) \rangle = \frac{1}{S} \langle \int P(\vec{x})P(\vec{x} + \vec{\rho}) \exp(i[\Phi(\vec{x}) - \Phi(\vec{x} + \vec{\rho})]) d\vec{x} \rangle \quad (5)$$

The characteristic function of a gaussian centered variable as Φ allows us to define the phase structure function and to write the Eq. 5 as:

$$\langle \vec{B}(\vec{\rho}) \rangle = \frac{1}{S} \int P(\vec{x})P(\vec{x} + \vec{\rho}) \exp\left(-\frac{1}{2}D_{\Phi}(\vec{x}, \vec{\rho})\right) d\vec{x} \quad (6)$$

$$D_{\Phi}(\vec{x}, \vec{\rho}) = \langle |\Phi(\vec{x}) - \Phi(\vec{x} + \vec{\rho})|^2 \rangle \quad (7)$$

D_{Φ} is the phase structure function. The phase in the Kolmogorov model being stationary, D_{Φ} only depends on the separation in the pupil ρ and the Fried parameter r_0 . Roddier (1981)² gives us the theoretical value for the phase structure function:

$$D_{\Phi}(\vec{x}, \vec{\rho}) = D_{\Phi}(\vec{\rho}) = 6.88 \left(\frac{\rho}{r_0}\right)^{5/3} \quad (8)$$

Thus Eq. 6 simplifies:

$$\langle \vec{B}(\vec{\rho}) \rangle = \underbrace{\exp\left(-\frac{1}{2}D_{\Phi}(\vec{\rho})\right)}_{\vec{B}_{atm}(\vec{\rho})} \underbrace{\frac{1}{S} \int P(\vec{x})P(\vec{x} + \vec{\rho})d\vec{x}}_{\vec{B}_{tel}(\vec{\rho})} \quad (9)$$

$$\vec{B}_{atm}(\vec{\rho}) = \exp\left[-3.44 \left(\frac{\rho}{r_0}\right)^{5/3}\right] \quad (10)$$

The PSF is then simply the inverse Fourier transform of the OTF.

2.3 Long exposure PSF with AO

The equations are not modified by introducing an adaptive optics system. AO partially corrects the turbulent phase so that low spatial frequencies are filtered. This correction is not perfect and a residual phase ($\Phi_{\epsilon} = \Phi_{atm} - \Phi_{mirror}$) is still present. The major problem by introducing an AO is that, since the phase is filtered, the stationarity of the phase on the pupil is questionable. So, the OTF cannot be expressed as the product of the perfect telescope OTF and the atmospheric one.

$$\langle \vec{B}(\vec{\rho}) \rangle = \frac{1}{S} \int P(\vec{x})P(\vec{x} + \vec{\rho}) \langle \exp(i[\Phi_{\epsilon}(\vec{x}) - \Phi_{\epsilon}(\vec{x} + \vec{\rho})]) \rangle d\vec{x} \quad (11)$$

$$= \frac{1}{S} \int P(\vec{x})P(\vec{x} + \vec{\rho}) \exp\left(-\frac{1}{2}D_{\Phi_{\epsilon}}(\vec{x}, \vec{\rho})\right) d\vec{x} \quad (12)$$

$$D_{\Phi_{\epsilon}}(\vec{x}, \vec{\rho}) = \langle |\Phi_{\epsilon}(\vec{x}) - \Phi_{\epsilon}(\vec{x} + \vec{\rho})|^2 \rangle \quad (13)$$

Because of the integral term that depends on the spatial variable \vec{x} , the OTF cannot be computed easily. Indeed, this computation require a large number of pixel per pixel shifts for each phase screen (30 000 to ensure convergence of the OTF). To accelerate the computation, Conan (1995)³ propose to spatially average on the pupil the residual phase so that the phase structure function does not depend anymore on \vec{x} . Thus,

$$\overline{D}_{\Phi_{\epsilon}}(\vec{\rho}) = \frac{\int P(\vec{x})P(\vec{x} + \vec{\rho})D_{\Phi_{\epsilon}}(\vec{x}, \vec{\rho})d\vec{x}}{\int P(\vec{x})P(\vec{x} + \vec{\rho})d\vec{x}} \quad (14)$$

As a consequence,

$$\langle \vec{B}(\vec{\rho}) \rangle = \underbrace{\exp\left(-\frac{1}{2}\overline{D}_{\Phi_{\epsilon}}(\vec{\rho})\right)}_{\vec{B}_{\epsilon}(\vec{\rho})} \underbrace{\frac{1}{S} \int P(\vec{x})P(\vec{x} + \vec{\rho})d\vec{x}}_{\vec{B}_{tel}(\vec{\rho})} \quad (15)$$

This approximation will be analyzed in Sec. 4.

3. LONG EXPOSURE AO PSF RECONSTRUCTION

As explain in Sec. 1, our aim is to estimate the PSF during the observation using the data from the AO-loop. In this section, inspired by V eran et al. (1997),¹ we remember the basics of the reconstruction.

The residual phase, the atmospheric part of the PSF, can be split into two terms: the mirror phase (low frequencies measured and corrected by the system) and the orthogonal phase (high frequencies not measured by the system).

$$\Phi_{\epsilon}(\vec{x}) = \epsilon_{\parallel}(\vec{x}) + \epsilon_{\perp}(\vec{x}) \quad (16)$$

Following this decomposition, the stationnarized residual phase structure function is the sum of three terms :

$$\overline{D}_{\Phi_{\epsilon}}(\vec{\rho}) = \overline{D}_{\epsilon_{\parallel}}(\vec{\rho}) + \overline{D}_{\epsilon_{\perp}}(\vec{\rho}) + 2\Gamma_{\epsilon}(\vec{\rho}) \quad (17)$$

Where,

$$\overline{D}_{\epsilon_{\parallel}}(\vec{\rho}) = \langle |\epsilon_{\parallel}(\vec{x}) - \epsilon_{\parallel}(\vec{x} + \vec{\rho})|^2 \rangle \quad (18)$$

$$\overline{D}_{\epsilon_{\perp}}(\vec{\rho}) = \langle |\epsilon_{\perp}(\vec{x}) - \epsilon_{\perp}(\vec{x} + \vec{\rho})|^2 \rangle \quad (19)$$

$$\Gamma_{\epsilon}(\vec{\rho}) = \langle (\epsilon_{\parallel}(\vec{x}) - \epsilon_{\parallel}(\vec{x} + \vec{\rho}))(\epsilon_{\perp}(\vec{x}) - \epsilon_{\perp}(\vec{x} + \vec{\rho})) \rangle \quad (20)$$

$\Gamma_{\epsilon}(\vec{\rho})$ represents the correlation structure function between the orthogonal and the parallel phase. This term is non-null (because of the aliasing) but is considered as negligible. Indeed, we expect that the correlation between high frequencies and low spatial frequencies is negligible. This approximation will be analyzed in Sec. 4.

Thus, if $\Gamma_{\epsilon}(\vec{\rho}) = 0$, the OTF is:

$$\langle \vec{B}(\vec{\rho}) \rangle = \underbrace{\exp\left(-\frac{1}{2}D_{\epsilon_{\parallel}}(\vec{\rho})\right)}_{\vec{B}_{\epsilon_{\parallel}}} \underbrace{\exp\left(-\frac{1}{2}D_{\epsilon_{\perp}}(\vec{\rho})\right)}_{\vec{B}_{\epsilon_{\perp}}} \vec{B}_{tel}(\vec{\rho}) \quad (21)$$

3.1 Estimation of $\overline{D}_{\epsilon_{\parallel}}$

Let's consider a simple model of AO, as describe Fig. 1.

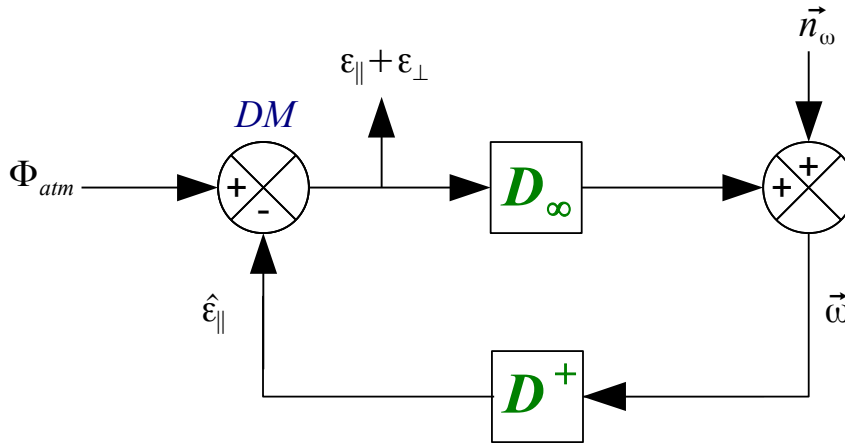


Figure 1. Simple model of an adaptive optics loop model

\mathbf{D}_{∞} is the theoretical interaction block matrix containing an infinity of columns, defined such as $\mathbf{D}^{\infty} = [\mathbf{D}_{\parallel}, \mathbf{D}_{\perp}]$, and \mathbf{D}^+ , the modal control matrix defined such as $\mathbf{D}^+ = (\mathbf{D}_{\parallel}^t \mathbf{D}_{\parallel})^{-1} \mathbf{D}_{\parallel}^t$ and \mathbf{D}_{\parallel} the real interaction matrix of mirror modes. $\vec{\omega}$ is the vector of measurements, $\hat{\epsilon}_{\parallel}$ is the reconstructed parallel phase by the DM and \vec{n}_{ω} is the vector of noise in the measurement space. Using this model, the real measures are expressed as:

$$\vec{\omega} = \mathbf{D}_{\infty}(\epsilon_{\parallel} + \epsilon_{\perp}) + \vec{n}_{\omega} \quad (22)$$

$$= \mathbf{D}_{\parallel}\epsilon_{\parallel} + \mathbf{D}_{\perp}\epsilon_{\perp} + \vec{n}_{\omega} \quad (23)$$

$$= \mathbf{D}_{\parallel}\epsilon_{\parallel} + \vec{a} + \vec{n}_{\omega} \quad (24)$$

Where $\vec{a} = \mathbf{D}_{\perp}\epsilon_{\perp}$ is the vector of the aliasing contribution on the measurements. Thus the reconstruction using the least-square estimator is written as:

$$\mathbf{D}^+ \vec{\omega} = \underbrace{\mathbf{D}^+ \mathbf{D}_{\parallel}}_1 \epsilon_{\parallel} + \mathbf{D}^+ \vec{a} + \mathbf{D}^+ \vec{n}_{\omega} \quad (25)$$

And we obtain the instantaneous parallel phase estimation (decomposed on the mirror modes):

$$\hat{\epsilon}_{\parallel}(t) = \mathbf{D}^+(\vec{\omega} - \vec{n}_{\omega}) - \mathbf{D}^+ \vec{a} = \mathbf{D}^+ \vec{\omega} - \mathbf{D}^+ \vec{a} \quad (26)$$

$$= \sum_i^N \epsilon_i(t) M_i(\vec{x}) \quad (27)$$

$\vec{\omega}$ is the non noisy measures.

So, to estimate the residual parallel phase structure function, we want to compute:

$$\overline{D}_{\epsilon_{\parallel}} = \sum_i \sum_j \langle \hat{\epsilon}_{\parallel} \hat{\epsilon}_{\parallel}^t \rangle_{ij} U_{ij}(\vec{\rho}) \quad (28)$$

With, following the previous equations:

$$\langle \hat{\epsilon}_{\parallel} \hat{\epsilon}_{\parallel}^t \rangle = \mathbf{D}^+(\langle \dot{\omega} \dot{\omega}^t \rangle - \langle aa^t \rangle - \langle \dot{\omega} a^t \rangle - \langle a \dot{\omega}^t \rangle) \mathbf{D}^{+t} \quad (29)$$

$$U_{ij}(\vec{\rho}) = \frac{\int P(\vec{x}) P(\vec{x} + \vec{\rho}) [M_i(\vec{x}) - M_i(\vec{x} + \vec{\rho})] [M_j(\vec{x}) - M_j(\vec{x} + \vec{\rho})] d\vec{x}}{\int P(\vec{x}) P(\vec{x} + \vec{\rho}) d\vec{x}} \quad (30)$$

The equation 29 introduces two cross-terms: $\langle \dot{\omega} a^t \rangle$ and its transpose $\langle a \dot{\omega}^t \rangle$. These terms will not be studied later since Véran et al. (1997)¹ fully describe its behavior. Moreover, this term become $\langle \dot{\omega} a^t \rangle \simeq - \langle aa^t \rangle$ when the bandwidth of the system is large enough. So, we obtain:

$$\langle \hat{\epsilon}_{\parallel} \hat{\epsilon}_{\parallel}^t \rangle_{ij} = \mathbf{D}^+(\langle \dot{\omega} \dot{\omega}^t \rangle + \langle aa^t \rangle) \mathbf{D}^{+t} \quad (31)$$

$$\langle \dot{\omega} \dot{\omega}^t \rangle = \langle \omega \omega^t \rangle - C_{n_w} \quad (32)$$

Since we need the non-noisy measures, we have to get a clean estimation of the noise variance during the observation.

3.2 Estimation of the aliasing

The aliasing on the measurements is caused by high frequencies in the turbulent phase misinterpreted by the WFS. This effect gives us a non-null measurement, reconstructed by the computer and compensated by the DM, introducing an aliased phase. However, alike the orthogonal component, the aliasing can be estimated using Monte-Carlo simulations by filtering low spatial frequencies in the introduced phase. The measure of the aliasing can be estimated with:

$$\langle aa^t \rangle \Big|_{\frac{D}{r_0}} = \langle aa^t \rangle \Big|_{\frac{D}{r_0}=1} \left(\frac{D}{r_0} \right)^{5/3} \quad (33)$$

$\langle aa^t \rangle \Big|_{\frac{D}{r_0}=1}$ is computed by simulations and this estimation will be studied Sec. 4.4.

3.3 Noise variance estimation

To reconstruct the PSF following Eq. 29, we need an accurate estimation of the noise variance on the measures. This problem was fully studied by Gendron & Léna (1994, 1995)^{4,5} which described three methods to estimate the noise variance on the measurements: the power spectrum density, the auto-correlation and the curl method. The latter was not used in our study and the PSD and the auto-correlation method gives approximately the same estimation of the noise variance (see Fig. 2).

In this study, while the noise introduced on the measurements can be considered as stationary white gaussian, in the mirror space, the filtered noise is no more stationary (Gendron & Léna 1994),⁴ as a result, the AO corrected residual phase is not fully stationary. the impact of the noise variance estimation on the reconstructed OTF is studied in Sec. 4.

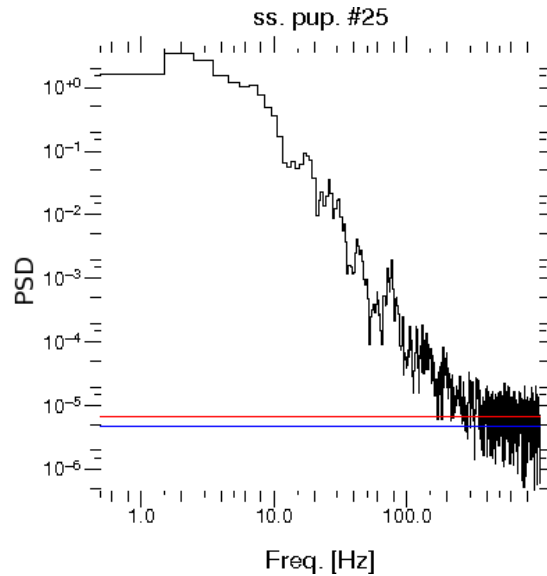


Figure 2. Noise variance estimation using the PSD (*red*) and the auto-correlation method (*blue*) superimposed on the PSD measurements on the sub-pupil #25 (on the pupil edge) with respect to the frequency.

4. APPROXIMATION ANALYSIS

In this section, we present the effect on the OTF of the main approximations which contribute on the error on the PSF reconstruction using simple simulations.

4.1 The AO system model and simulation

Yao* (Yorick Adaptive Optics) was used for realistic end-to-end AO simulations. To accelerate the simulation process, we simulated a rather small system consisting on a 6×6 sub-apertures WFS (Shack-Hartmann) and a 7×7 actuator DM. For each iteration, we compute the different phase structure functions and save the circular buffers of the required measures.

4.2 The approximation of the stationary phase

To estimate the effect of the stationary phase approximation, we need to compute the exact OTF. However, to optimized the computation time, we need to use a simplified simulations (no WFS and a Zernike DM). The simulation consists in a turbulent screen phase moving into one direction. The phase is then projected on the Zernike basis and the parallel component is subtracted of the phase screen. We vary four parameters: the Fried parameter r_0 , the noise level, the loop gain, and the number of corrected Zernike modes for 30 000 loop iterations and a loop gain equal to 1. The gain is here define as a scaling factor on the Kolmogorov statistics. if the gain is set to 0.7, 70% of the variance of the phase is filtered in each mode Fig. 7 shows the result for different set of parameters.

As shown in Fig. ??, in most cases the stationary phase approximation has no impact on the OTF. The OTF is not changed by varying r_0 (Fig. ?? top left) or by varying the AO loop gain (Fig. ?? top right), or by varying the number of Zernike despite the difference at very low Strehl ($\sim 1\%$) but this is caused by the numerical precision of our method to compute the exact OTF (Fig. ?? bottom left). Bottom right, we can see that at low Strehl ($\leq 10\%$), the residual phase is no more stationary. Indeed, the noise, in the modes space, follows a power law such as $(N + 1)^{-2}$ that is different to the turbulence law that is $(N + 1)^{-11/3}$ for the highest order modes (N is the Zernike number). Thus, the variance of the noise is superior to the turbulence variance, introducing the non-stationarity in the OTF computation.

*<http://frigaut.github.com/yao/index.html>

4.3 The global cross-term Γ_ϵ

Γ_ϵ is a coupling term (see Eq. 20) between the orthogonal phase and the residual parallel phase. The aliasing in ϵ_{\parallel} is the main contributor to the correlation between high/low spatial frequencies. The Fig. 3 indicates that only the high frequencies in the image are affected by the Γ_ϵ term (the oscillation at low frequency is negligible compared to the high frequency). This is also an effect of the aliasing because the aliased frequencies affects the highest frequencies measured by the system.

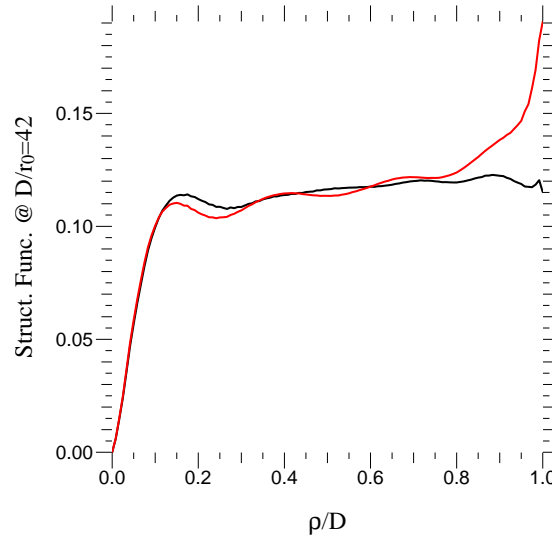


Figure 3. Circular average of the Γ_ϵ term contribution to \overline{D}_ϵ . *Black*: \overline{D}_ϵ , *red*: structure function approximated.

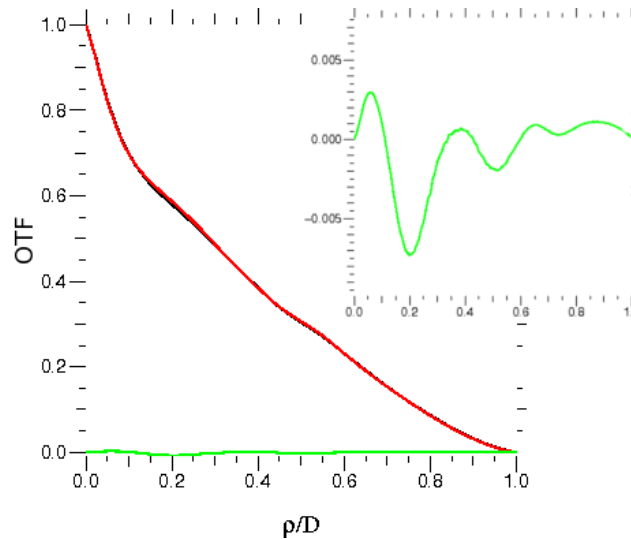


Figure 4. Circular average of the Γ_ϵ term contribution to the OTF for a Strehl ratio of 20%. *Black*: the real OTF of the observation, *red*: by neglecting the cross-term and *green*: the difference between the real and the incomplete one.

Its effect on the OTF is negligible (Fig. 4), even for a rather low Strehl ratio. As a consequence, the PSF is marginally affected by this approximation.

4.4 Aliasing

The aliasing on the measurements needs to be estimated using a simulation at $D/r_0 = 1$ and then rescaled using Eq. 33. This rescaling requires the knowledge of the Fried parameter r_0 and we show Fig. 5 that a relative error of 30% on r_0 has no significant impact on the reconstructed OTF.

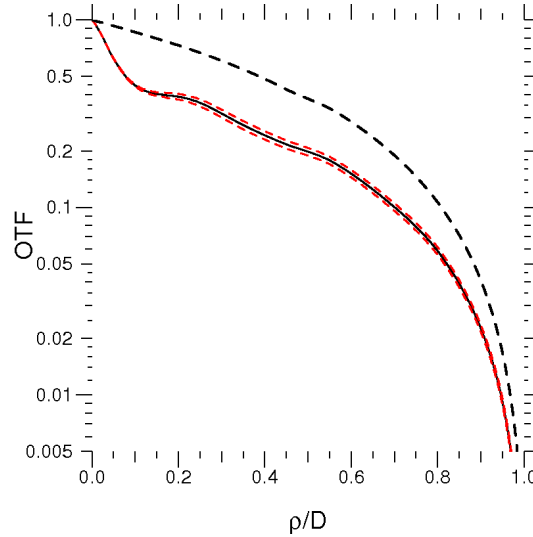


Figure 5. The aliasing estimation error. The upper black dashed line is the perfect telescope circular averaged OTF. The black solid line is the reconstructed OTF with the real aliasing obtained by simulation. The red dashed curve are the reconstructed OTF by over/under estimating r_0 by 30%.

4.5 The noise estimation

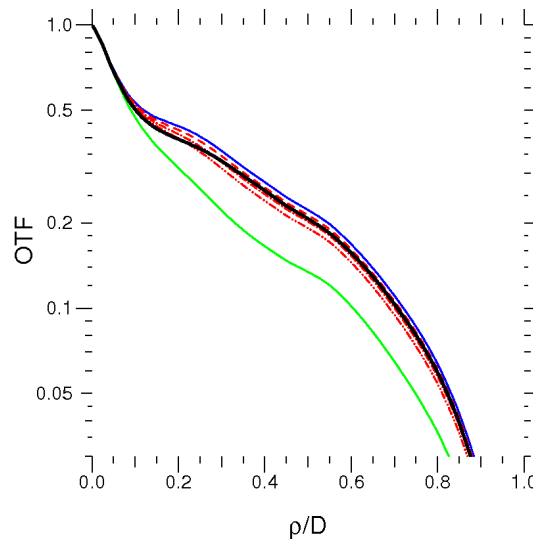


Figure 6. OTF reconstruction (circular averaged) and impact of the noise variance estimation. *Black*: the real simulated OTF. *Blue*: reconstructed OTF with the non-noisy measurements. *Green*: reconstructed OTF with the noisy measurements. *Red*: reconstruction of the OTF with a relative error on the noise variance estimation of 10%, 20% and 30%.

Sec. 4.2 we concluded that the noise variance is important for the stationarity of the residual phase. We show

that it is as well important in the OTF reconstruction (Fig. 6). Indeed, an error on the noise variance induced an error on the measurements covariance matrix (Eq. 26).

We can see (Fig. 6) that the noisy measurements cannot be used to reconstruct the OTF (green line) because the reconstruction is very different of the real one. With the subtraction of the noise variance, we reconstruct the OTF with a rather good precision (blue line). However, with 30% of relative error on the noise variance estimation, the error on the OTF becomes critical. Indeed, the Strehl ratio between the reconstruction using non-noisy data and the noisy data with 30% error on noise variance is different of $\sim 10\%$ (for a simulated Strehl ratio of 50%). For a relative error up to 20% on the noise variance, the error on the OTF is moderate, leading to an error of a few percent on the Strehl ratio.

5. CONCLUSION AND PERSPECTIVE

In this paper, we conclude that the main approximations that are done during the PSF reconstruction process are valid for a Shack-Hartmann WFS for normal performances of an adaptive optics system (Strehl $> 10\%$).

It is necessary, to reproduce the structure function of the phase, at high spatial frequency to implement the computation of the global cross-term. However, we show that the global cross-term Γ_ϵ has no effect on the OTF/PSF and can be neglected.

Moreover, the stationary phase approximation is as well valid for this range of performances. We show that the noise on the measurements is the main contributor to this approximation by introducing non stationary component in the phase of the mirror as well as the bandwidth error of the system (not studied in this paper).

The noise is as well important in the reconstruction process since it is necessary to obtain the non-noisy measurements. Using the noisy measurements, we are unable to reconstruct the OTF. We show that for a relative error superior to 10% on the noise variance estimation, the Strehl ratio is underestimated of a few percent. For a relative error of $\sim 30\%$, the error becomes significant ($>10\%$ on the Strehl ratio).

The estimation of the aliasing on measurements using simulations introduced moderate errors on the reconstruction process, even for a relative error of 30% on the estimation of the r_0 parameter. But the aliasing is crucial and need to be taken into account in the PSF reconstruction.

For the future, we want to implement the computation of the different errors to feed a myopic deconvolution algorithm, such as describe in Mugnier et al. (2004),⁶ allowing one to perform an accurate astrometry/photometry on the observed objects and to strengthen the contrast in the images, even for poor Strehl ratios during the observation.

ACKNOWLEDGMENTS

The author would like to thank Eric Gendron for its precious help on the noise determination using the curl method, and Céline Guédé for the inspiration of the poster.

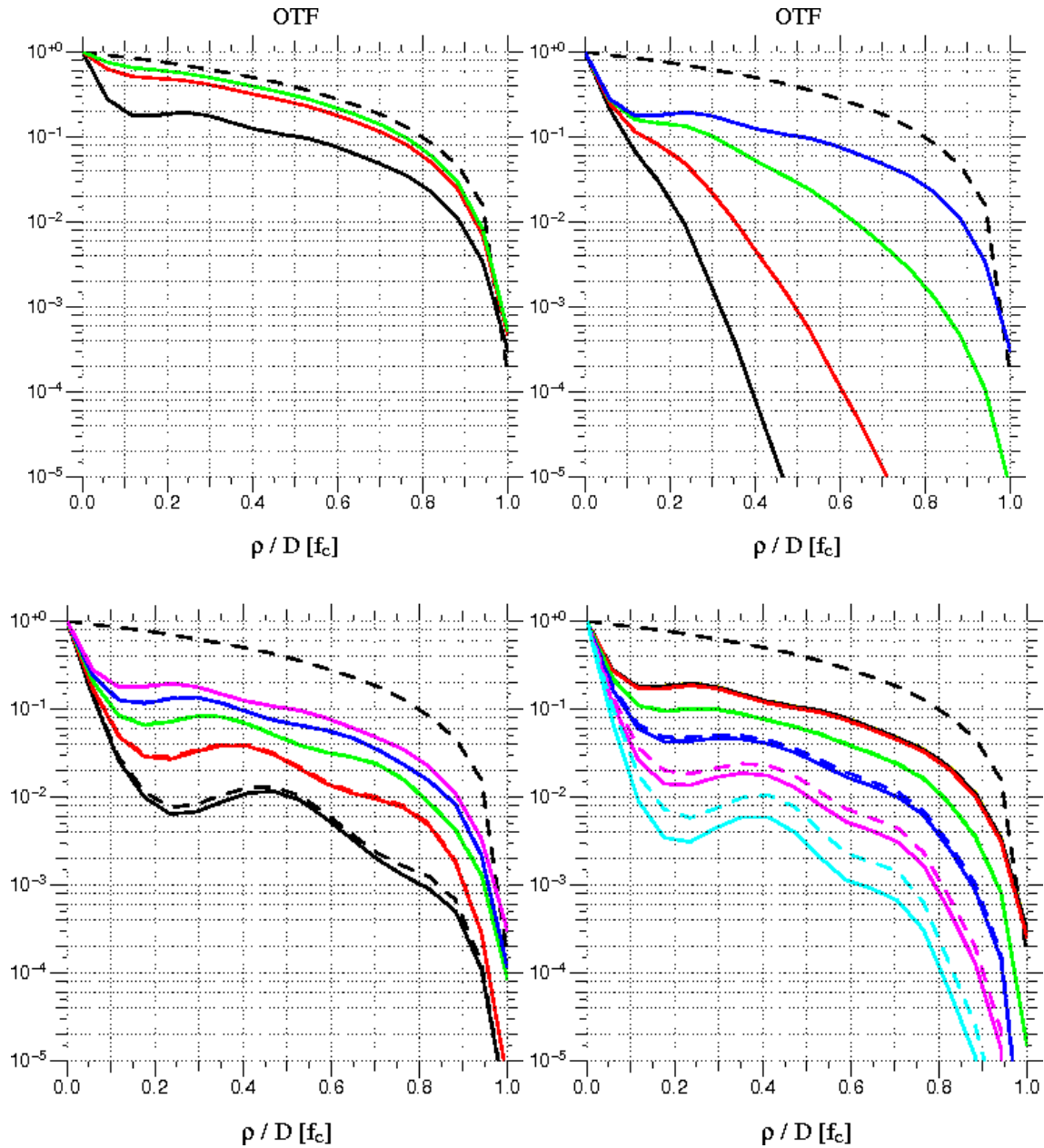


Figure 7. Plots representing the effect of the different parameters on the stationary phase approximation. All lines represent circular averaged OTF. The dashed lines represent the exact OTF, the solid lines represent the OTF with the stationary phase approximation. The upper black dashed line is the OTF of the perfect telescope. *Top left:* OTFs varying the Fried parameter ($\frac{D}{r_0} = 16, 8$ and 5 respectively *black, red* and *green*) for a simulation with no noise, 36 corrected Zernike and a gain equal to 1. *Top right:* OTFs varying the gain of the AO loop (for a gain of 0.7, 0.8, 0.9 and 1 respectively *black, red, green* and *blue*) for a $\frac{D}{r_0} = 16$, 36 corrected Zernike and no noise in the simulation. *Bottom left:* OTFs where the number of corrected Zernike vary (correction with 10, 15, 21, 28, and 36 Zernike respectively *black, red, green, blue* and *magenta*) for a simulation at $\frac{D}{r_0} = 16$, no noise and a loop gain of 1. *Bottom right:* the OTFs varying the noise level (for a noise of 10^{-2} , 8×10^{-3} , 6×10^{-3} , 4×10^{-3} and 10^{-3} times the the turbulence variance respectively *cyan, magenta, blue, green* and *red*) at $\frac{D}{r_0} = 16$, a loop gain of 1 and 36 corrected Zernike. In each plot where the dashed line is not visible, it is superimposed to the solid one

REFERENCES

- [1] Véran, J.-P., Rigaut, F., Maitre, H., & Rouan, D., “Estimation of the adaptive optics long-exposure point-spread function using control loop data,” *J. Opt. Soc. Am. A* **14** (Nov. 1997).
- [2] Roddier, F., “The effects of atmospheric turbulence in optical astronomy,” *Progress in optics. Volume 19. Amsterdam, North-Holland Publishing Co., 1981, p. 281-376.* **19**, 281–376 (1981).
- [3] Conan, J.-M., *Etude de la correction partielle en optique adaptative*, PhD thesis, Université Paris XI, Orsay, France (1995).
- [4] Gendron, E. & Léna, P., “Astronomical adaptive optics. 1: Modal control optimization,” *Astronomy and Astrophysics* **291**, 337–347 (Nov. 1994).
- [5] Gendron, E. & Léna, P., “Astronomical adaptive optics. II. Experimental results of an optimized modal control,” *Astronomy and Astrophysics Supplement* **111**, 153 (May 1995).
- [6] Mugnier, L. M., Fusco, T., & Conan, J.-M., “MISTRAL: a myopic edge-preserving image restoration method, with application to astronomical adaptive-optics-corrected long-exposure images,” *J. Opt. Soc. Am. A* **21**, 1841–1854 (Oct. 2004).